The EMBO Journal (2011) 30, 2233–2245 | © 2011 European Molecular Biology Organization | Some Rights Reserved 0261-4189/11
www.embojournal.org

THE EMBO JOURNAL

EMBO open

Differential control of Eg5-dependent centrosome separation by Plk1 and Cdk1

Ewan Smith[1], Nadia Hégarat[1], Clare Vesely[1], Isaac Roseboom[2], Chris Larch[3], Hansjörg Streicher[3], Kornelis Straatman[4], Helen Flynn[5], Mark Skehel[5], Toru Hirota[6], Ryoko Kuriyama[7] and Helfrid Hochegger[1,*]

[1]Genome Damage and Stability Centre, University of Sussex, Brighton, UK, [2]Department of Physics and Astronomy, University of Sussex, Brigthon, UK, [3]Department of Chemistry and Biochemistry, University of Sussex, Brighton, UK, [4]Department of Biochemistry, University of Leicester, Leicester, UK, [5]CRUK London Research Institutes Clare Hall, South Mimms, UK, [6]The Cancer Institute, Japanese Foundation for Cancer Research, Ariake, Tokyo, Japan and [7]Department of Genetics, Cell Biology and Development, University of Minnesota, Minneapolis, MN, USA

Cyclin-dependent kinase 1 (Cdk1) is thought to trigger centrosome separation in late G2 phase by phosphorylating the motor protein Eg5 at Thr927. However, the precise control mechanism of centrosome separation remains to be understood. Here, we report that in G2 phase polo-like kinase 1 (Plk1) can trigger centrosome separation independently of Cdk1. We find that Plk1 is required for both C-Nap1 displacement and for Eg5 localization on the centrosome. Moreover, Cdk2 compensates for Cdk1, and phosphorylates Eg5 at Thr927. Nevertheless, Plk1-driven centrosome separation is slow and staggering, while Cdk1 triggers fast movement of the centrosomes. We find that actin-dependent Eg5-opposing forces slow down separation in G2 phase. Strikingly, actin depolymerization, as well as destabilization of interphase microtubules (MTs), is sufficient to remove this obstruction and to speed up Plk1-dependent separation. Conversely, MT stabilization in mitosis slows down Cdk1-dependent centrosome movement. Our findings implicate the modulation of MT stability in G2 and M phase as a regulatory element in the control of centrosome separation.

The EMBO Journal (2011) **30,** 2233–2245. doi:10.1038/emboj.2011.120; Published online 26 April 2011
Subject Categories: cell & tissue architecture; cell cycle
Keywords: actin; Eg5; microtubules; mitosis; Polo kinase

*Corresponding author. Genome Damage and Stability Centre, University of Sussex, Falmer, Brighton, East Sussex BN1 9RQ, UK. Tel.: +44 01 27 387 7510; Fax: +44 01 27 367 8121; E-mail: hh65@sussex.ac.uk

Received: 3 February 2011; accepted: 25 March 2011; published online: 26 April 2011

Introduction

Centrosomes are microtubule (MT)-nucleating centres in animal cells that need to be duplicated during each S phase and are separated during the G2/M transition to form the poles of the mitotic spindle (Blagden and Glover, 2003; Rosenblatt, 2005). Centrosome separation is a complex and poorly understood process that is of pivotal importance for chromosome stability. Inaccuracies in the control of centrosome separation can cause mono- and multipolar mitotic spindles and could be the cause of genomic instability (Ganem *et al*, 2009) and cancer (Basto *et al*, 2008; Castellanos *et al*, 2008). Separation is initiated by disjunction of the cohesive structures that link the two centriole pairs (Bornens *et al*, 1987; Paintrand *et al*, 1992). The distantly related proteins Rootletin and C-Nap1 appear to constitute the molecular core of this structure (Fry *et al*, 1998; Mayor *et al*, 2000; Bahe *et al*, 2005). Loss of cohesion is thought to involve Nek2 kinase (Fry *et al*, 1998), which has recently been shown to be targeted by the Hippo pathway (Mardin *et al*, 2010). Following disjunction, centrosomes are pushed apart by the force of MT-dependent motor proteins. This occurs at the very beginning of M phase at about the time of nuclear envelope breakdown (NEBD). The plus-end-directed MT motor Eg5 is clearly essential for centrosome separation across species (Le Guellec *et al*, 1991; Hagan and Yanagida, 1992; Hoyt *et al*, 1992; Roof *et al*, 1992; Sawin *et al*, 1992; Heck *et al*, 1993). Various obstructions have been reported to impede Eg5 activity (Mountain *et al*, 1999; Tanenbaum *et al*, 2008; Woodcock *et al*, 2010) and centrosomes in interphase cells are also subjected to forces that ensure positioning of the organelle in the cell centre (Burakov *et al*, 2003; Zhu *et al*, 2010). How centrosome disjunction, separation and positioning are coordinated at the G2/M transition to allow timely formation of the spindle poles remains to be determined.

Centrosome separation is under stringent control by mitotic kinases, such as cyclin-dependent kinase 1 (Cdk1), polo-like kinase 1 (Plk1), Aurora A and Nek2, but it remains to be shown in detail how these kinases contribute to this process. Cdk1 has been attributed a central role in controlling centrosome dynamics (Meraldi and Nigg, 2002; Lim *et al*, 2009). It is unclear, if Cdk1 contributes to disjunction, but Cdk1 is thought to trigger separation by activating Eg5 (Blangy *et al*, 1995). Cdk1 phosphorylates Eg5 in its C-terminal tail domain at Thr927 stimulating its binding to MTs (Blangy *et al*, 1995; Cahu *et al*, 2008). Conversely, several recent studies suggest that Cdk1 may not be essential for centrosome separation (McCleland and O'Farrell, 2008; Gavet and Pines, 2010). Thus, Cdk1 function in centrosome separation remains to be firmly established.

Plk1 is another mitotic kinase that has been implicated in regulating bipolar spindle formation (Petronczki *et al*, 2008). Polo kinase was originally discovered as a *Drosophila* mutant with defective centrosomes and monopolar spindles (Sunkel and Glover, 1988). Plk1 contributes to accumulation of γ-tubulin at the centrosomes (Lane and Nigg, 1996; Casenghi *et al*, 2003; Oshimori *et al*, 2006) and stabilization of stable MT-kinetochore attachments (Sumara *et al*, 2004). Using Plk1 inhibitors or siRNA-mediated depletion results in collapsed spindles, with centrosomes in close proximity at the spindle equator (Sumara *et al*, 2004; van Vugt *et al*, 2004; McInnes *et al*, 2006; Lenart *et al*, 2007). However, a direct role for Plk1 in centrosome disjunction and/or separation remains to be established. In this study, we aimed to investigate the role of Cdk1 and Plk1 in triggering centrosome separation.

Results

Centrosome separation occurs in Cdk1-inhibited cells and depends on Plk1 and Eg5 activity

To clarify the role of Cdk1 in centrosome separation, we took advantage of a *cdk1as* DT40 cell line that carries an analogue-sensitive mutation in Cdk1 (*cdk1as* cells). In these cells, the mutant Cdk1 can be inhibited with high specificity by addition of the bulky ATP analogue, 1NMPP1, resulting in a late G2 phase arrest (Figure 1C), while the ATP analogue has no effect on the cell cycle of cells expressing WT Cdk1 (Hochegger *et al*, 2007). We found that, despite Cdk1 inhibition, centrosomes were clearly separated in about 60% of the 1NMPP1-treated *cdk1as* cells (Figure 1A and B). To confirm this result in a different experimental system, we used a chemical Cdk1 inhibitor, RO3306 (Vassilev *et al*, 2006), in *HeLa* cells, and found that approximately half of the RO3306-treated, G2-arrested cells (Figure 1F) displayed widely separated centrosomes (Figure 1D and E). To compare the timing of centrosome separation in the absence or presence of Cdk1 activity in more detail, we analysed centrosome separation in *cdk1as* cells that were pre-synchronized in G1 by elutriation and progressed to G2/M phase in the presence or absence of Cdk1 inhibition by 1NMPP1. Supplementary Figure S1A shows that centrosomes separated while cells progressed into G2/M. However, separation was delayed by approximately 2 h in the 1NMPP1-treated cells. We conclude from these results that Cdk1 is not strictly essential for centrosome separation, but is required for timely initiation of the process.

Next, we investigated the requirement of Plk1 in Cdk1-independent centrosome separation. We inhibited Plk1 using the BI2536 compound (Lenart *et al*, 2007) in combination with Cdk1 in DT40 and *HeLa* cells. Plk1 inhibition blocked centrosome separation in both chicken (Figure 1A and B) and human cells (Figure 1D and E). We analysed the centrioles in the BI2536/1NMPP1-treated *cdk1as* cells by transmission electron microscopy to rule out that Plk1 inhibition blocks centrosome replication in S phase. We could readily detect four centrioles in random sections in the Plk1-inhibited samples (Supplementary Figure S1B), suggesting that in these cells, centrioles had replicated, but centrosomes failed to separate. We also performed a parallel experiment in non-transformed human RPE cells expressing analogue-sensitive Plk1 (Burkard *et al*, 2007) to confirm that the inhibition of centrosome separation is a specific effect of Plk1 inhibition. Cdk1 inhibition by RO3306 blocked cells in both G1 and G2 phases, possibly due to a more central role of Cdk1 in S-phase progression in these cells. We marked late S/G2 cells by immuno-fluorescence using CENP-F antibodies (Varis *et al*, 2006) and scored these cells for separated centrosomes. G2-arrested Plk1WT-RPE cells treated with the ATP analogue 3MBPP1 displayed separated centrosomes in 90% of G2 cells, while the same treatment drastically reduced separation in *Plk1as*-RPE cells (Supplementary Figure S1C). These data suggest that Plk1 is required for Cdk1-independent centrosome separation in G2 phase.

To test the involvement of the motor protein Eg5 in Cdk1-independent centrosome separation, we used an improved monastrol derivate Trans24 (Sunder-Plassmann *et al*, 2005) to inhibit Eg5 in 1NMPP1-treated *cdk1as* cells, or the Eg5 inhibitor STLC (DeBonis *et al*, 2004) in the RO3306-treated *HeLa* cells. Strikingly, inhibition of Eg5 resulted in a drastic reduction of centrosome separation in G2-arrested DT40 (Figure 1A and B) and *HeLa* (Figure 1D and E) cells. Moreover, the distance between the few centrosomes that managed to separate was markedly decreased after both Plk1 and Eg5 inhibition (Figure 1B and E). Thus, by using different means of Cdk1, Plk1 and Eg5 inhibition, we found that Plk1 and Eg5 are required for Cdk1-independent centrosome separation in G2 phase in both chicken and human cells.

Cdk1 and Plk1 trigger centrosome separation independently, but with different dynamics

Current models of centrosome separation attribute a key role to Cdk1. Having established that Plk1 and Eg5 initiate centrosome separation independently of Cdk1, we wanted to address the effect of mitotic Cdk1 activation on the dynamics of both disjunction and separation. To address the differential impact of Cdk1 and Plk1 on centrosome separation, we compared the dynamics of centrosome separation following the activation of either Plk1 or Cdk1 using a series of synchronization and release experiments as described in Figure 2A. Briefly, we synchronized *cdk1as* cells in G2 phase with unseparated centrosomes by inhibiting both Cdk1 and Plk1 kinases. We subsequently removed either inhibitors or both together from the medium and followed centrosome separation over time by immuno-fluorescence. We found that release from the 1NMPP1 arrest in *cdk1as* cells was more effective and reproducible than the release from RO3306 (90% versus 20% of mitotic cells after 30 min of release; Xu *et al*, 2010) and thus decided to perform our analysis in the DT40 system. Remarkably, activation of both Cdk1 and Plk1 led to a burst of centrosome separation in the first 20 min after release in >90% of the cells. These cells readily entered mitosis and divided within an hour after release (Figure 2B; Supplementary Figure S2). The initial separation was still effective even in the presence of the Plk1 inhibitor. However, in these cells, the mitotic spindles were defective and cells remained arrested in mitosis (Supplementary Figure S2). The poles of the mitotic spindle appeared to collapse, having markedly decreased levels of γ-tubulin (compare enlarged γ-tubulin panels in Supplementary Figure S2). In marked contrast, Plk1-driven centrosome separation was ineffective and slow, reaching an average distance of 4 μm after 3 h (Figure 2B; Supplementary Figure S2).

In order to observe the dynamics of disjunction and separation in single cells, we performed a parallel experiment using 3D live cell imaging of GFP-γ-tubulin-expressing *cdk1as*

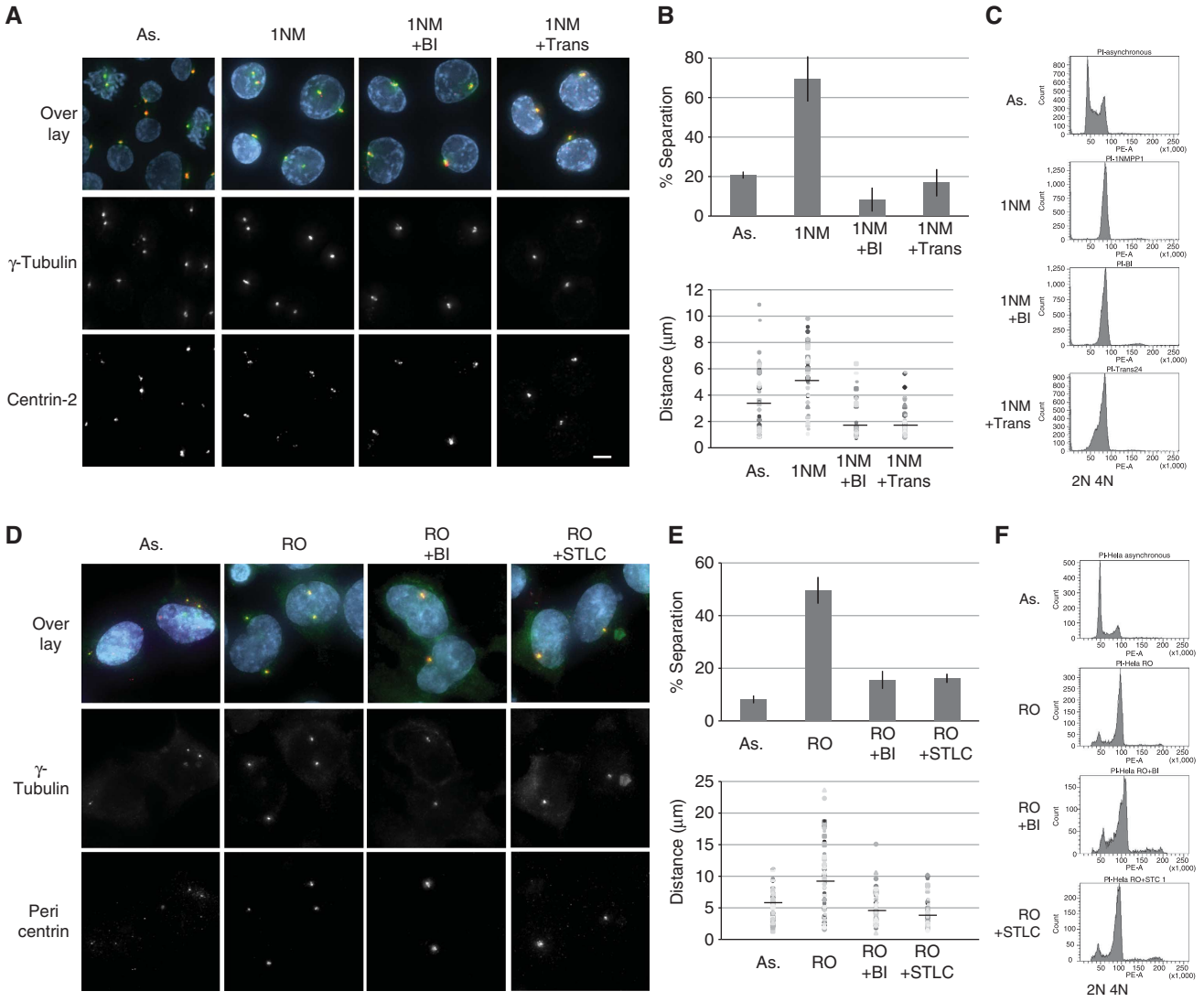

Figure 1 Cdk1-independent centrosome separation requires Plk1 and Eg5 activity. (**A**) DT40 *cdk1as* cells were analysed by immunofluorescence using anti-γ-tubulin and anti-centrin-2 antibodies and counterstained with DAPI. The panels display deconvolved maximum intensity projections (MIPs) of 3D images of representative samples (scale bar, 5 μm). Asynchronous cells are shown in the far left panel (As.). Cdk1 was inhibited by treating cells for 6 h with 10 μM 1NMPP1 (1NM). To inhibit Plk1, 100 nM of BI 2536 was added at the same time as 1NMPP1 (1NM + BI). To inhibit chicken Eg5, we added 33 μM trans-24 together with 1NMPP1 (1NM + Trans). (**B**) Quantitative analysis of centrosome separation using immuno-fluorescence and automated scanning microscope analysis (Olympus SCAN-R; see Material and methods). As., $N = 962$; 1NM, $N = 1300$; 1NM + BI, $N = 569$; 1NM + Trans, $N = 638$; error bars indicate the s.d. in three independent experiments. We scored centrosome distances in the same samples by analysing 3D images using IMARIS ($N = 50$); distances above 0.5 μm were scored as separated; results from individual cells are plotted; the bars show the mean distances (As., 3.4 μm; 1NM, 5.25 μm; 1NM + BI, 1.8 μm; 1NM + Trans, 1.84 μm). (**C**) PI staining and FACS analysis of same samples as in (**A**). (**D**) *HeLa* cells were analysed by immunofluorescence using anti-γ-tubulin, anti-pericentrin antibodies and DAPI. The panels display deconvolved MIPs of 3D images of representative samples (scale bar, 10 μM). Asynchronous cells are shown in the far left panel (As.). Cdk1 was inhibited by treating cells for 20 h with 7.5 μM RO3306 (RO). To inhibit Plk1, 100 nM of BI 2536 was added at the same time as RO 3066 (RO + BI). To inhibit human Eg5, we added 5 μM STLC together with RO3306 (RO + STLC). (**E**) Quantitative analysis of 3D images (% separation As., $N = 524$; RO, $N = 343$; RO + BI, $N = 415$; RO + STLC, $N = 380$; error bars indicate the s.d. in three independent experiments). Distances were scored in 3D images using Imaris ($N = 50$) as in (**B**); the bars indicate the mean distance; As., 5.7 μm; RO, 9.2 μm; RO + BI, 4.6 μm; RO + STLC, 4.1 μm. (**F**) FACS analysis of the indicated *HeLa* samples.

cells. Similar to the results described above, we observed a striking difference between centrosome separation triggered by Plk1 and Cdk1. If Cdk1 remained inactive, centrosome disjunction occurred on average an hour after release from BI2536 (Figure 3A and B; Supplement Movie S2). Moreover, movement of the centrosomes was not linear, but pulling and pushing forces appeared to compete with each other. We determined an average centrosome velocity of 0.04 μm/min in these cells. Activation of Cdk1 caused a dramatic change in dynamics of both disjunction and movement. The centrosomes came apart within minutes and had undergone considerable separation within the first 5 min after release (Figure 3A and B; Supplement Movie S1). The initial dynamics of Cdk1-driven centrosome separation were only modestly changed in the presence of the Plk1 inhibitor. Disjunction occurred with a brief delay at about 5 min after release, and the average velocity of separation was decreased from 1.1 μm/min when both Plk1 and Cdk1 were active to

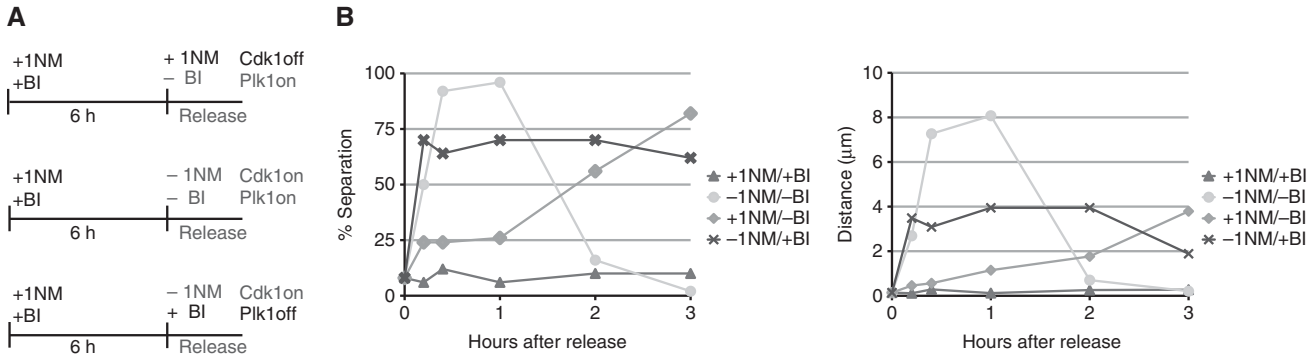

Figure 2 Dynamics of centrosome separation after release from inhibitors. (**A**) Experimental set-up. DT40 *cdk1as* cells were arrested in G2 with unseparated centrosomes by a 6-h co-treatment with 10 μM 1NMPP1 and 100 nM BI2536. Differential wash out of either inhibitor (three times in 50 ml containing either 10 μM 1NMPP1 or 100 nM BI2536), both inhibitors together or no inhibitor allowed us to follow centrosome separation triggered by Plk1, Cdk1 or both kinases in asynchronous population of cells. (**B**) Cells from the different release protocols were fixed at the indicated time points and analysed by immuno-fluorescence with anti-γ-tubulin and anti-α-tubulin antibodies and counter-stained with DAPI. 3D images were taken and centrosome separation and distances were scored using Imaris ($N > 100$ for each time point).

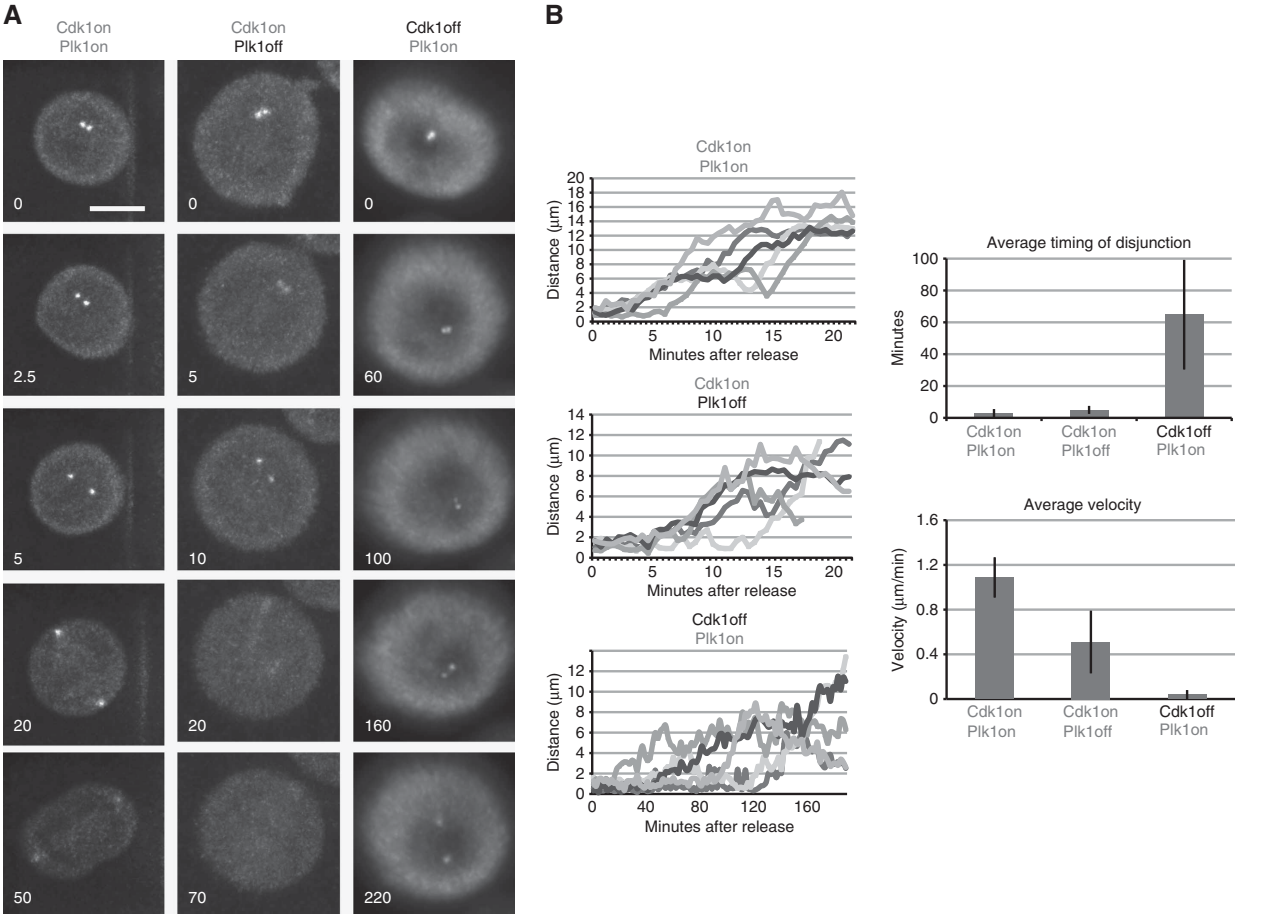

Figure 3 Dynamics of Plk1 and Cdk1 induced centrosome separation in live cells. (**A**) 3D time-lapse microscopy of differentially released *cdk1as* cells expressing GFP-γ-tubulin (see Materials and methods). The still images are MIPs of deconvolved 3D images (scale bar, 5 μm) from a time-lapse series (see also Supplementary Movies 01–03). (**B**) Quantification of centrosome distance for each release experiment. Distances were measured using Imaris in the deconvolved time-lapse series. Note the difference in the time scale between the different panels. Disjunction was defined as the first time point at which a distance of >1 μm was reached. Velocities were calculated as described in Materials and methods.

0.5 μm/min when Plk1 was kept shut off. Similar to our observations in Figure 2, Plk1 inhibition caused a dispersal of GFP-γ-tubulin from the centrosomes after NEBD and it became progressively harder to detect the GFP signal on the spindle poles (Figure 3A; Supplement Movie S3).

In summary, these data suggest that both Cdk1 and Plk1 are able to trigger centrosome separation, albeit with very different dynamics. Several questions arise from these observations. First, the role of Plk1 in centrosome separation needs to be clarified. Plk1 could act at the disjunction step,

control Eg5 activity or be involved in both processes. Second the difference in the speed of separation needs to be explained. In the absence of Cdk1 activity mutually opposing forces appear to act on the centrosome, resulting in a staggering to-and-fro movement. Once Cdk1 is active, centrosomes move rapidly and without apparent hindrance. This could be explained by the full activation of Eg5 by Cdk1, which could be sufficient to overcome the resistant force. Alternatively, Eg5 may already be fully primed for action in interphase and mitotic Cdk1 may act by down-regulating the Eg5-opposing forces. In this case, experimental elimination of these forces should be sufficient to speed up the process even in the absence of Cdk1 activity.

Plk1 acts both upstream and downstream of C-Nap1 displacement from the centrosomes

We first investigated the role of Plk1 in centrosome disjunction. This process is initially triggered by loss of cohesive proteins that hold the duplicated centriole pairs together. C-Nap1 has been reported to form the core of this structure and depletion of this protein is sufficient to trigger centrosome splitting (Mayor *et al*, 2000; Bahe *et al*, 2005). We reasoned that if Plk1 acts upstream of C-Nap1 displacement, this protein should still be present on the centrosomes when both Cdk1 and Plk1 are inhibited. Conversely, inhibition of Cdk1 alone should result in displacement of C-Nap1 from the centrosomes. Figure 4A shows that C-Nap1 is not detectable on centrosomes in RO3306-treated *HeLa* cells, while it is localized at centrosomes in cells treated with both Cdk1 and Plk1 inhibitors. Previous studies reported a decrease in C-Nap1 levels in mitotic cells (Mayor *et al*, 2002). It was reported that this reduction is not due to proteasome-dependent degradation of C-Nap1 but may be a consequence of mitotic-specific phosphorylation. We found that C-Nap1 levels were significantly reduced in Cdk1-inhibited cells compared with an asynchronous control (Figure 4B). However, Plk1 inhibition did not alter this reduction of C-Nap1 levels. These results suggest that while Plk1 acts specifically on the displacement of C-Nap1 from the centrosomes, the changes in total protein levels occur in G2 phase independently of both Plk1 and Cdk1.

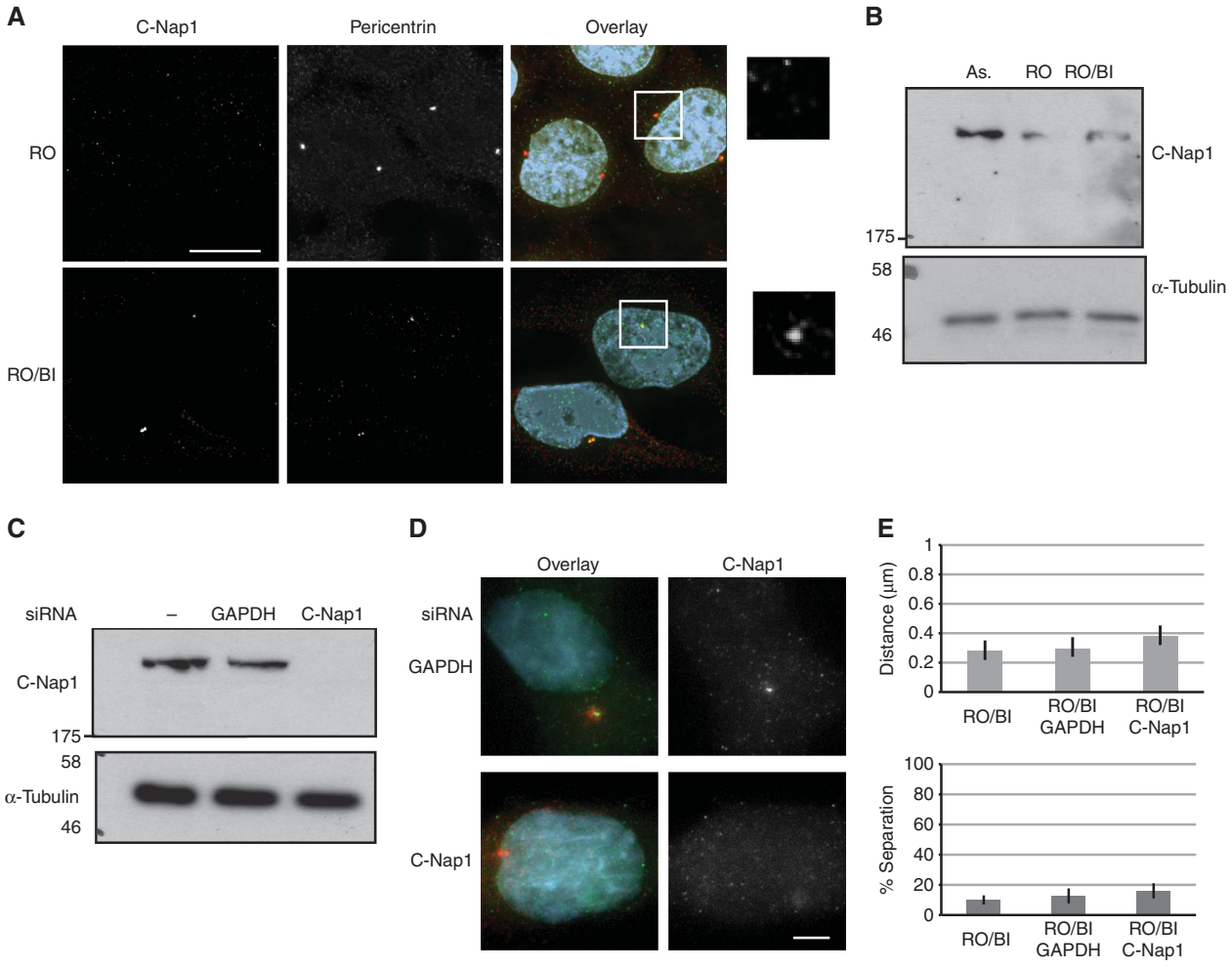

Figure 4 Plk1 triggers C-Nap1 displacement from centrosomes in Cdk1-inhibited cells. (**A**) Immuno-fluorescent staining of *HeLa* cells treated for 20 h with either 10 μM RO3306 or 10 μM RO3306 and 100 nM BI2536 with C-Nap1 and Pericentrin antibodies. Panels show MIPS of deconvolved 3D stacks (scale bar, 15 μm). The right panels show C-Nap1 staining of a magnified area around the centrosome as indicated. (**B**) C-Nap1 immuno-blots of *HeLa* cells treated as in (**A**). (**C**) Immuno-blot of C-Nap1 siRNA transfected and control cells with the indicated antibodies. (**D**) Confirmation of C-Nap1 knockdown by siRNA in RO3066-treated *HeLa* cells by immuno-fluorescence (scale bar, 5 μm). (**E**) Centrosome separation of C-Nap1 siRNA transfected and control cells. Separation and distances were scored from 3D stack images using Imaris. Shown are the mean values and s.d. of three independent experiments ($N > 100$ for each condition).

This involvement of Plk1 in centrosome disjunction could be sufficient to explain why centrosome separation is blocked by Plk1 inhibition. If this were true, artificial destruction of centrosome cohesion by C-Nap1 depletion should be sufficient to allow centrosome separation in the absence of Plk1 activity. We tested this hypothesis by knocking down C-Nap1 in cells treated with both the RO3306 and BI2536 inhibitors. Our siRNAs successfully depleted C-Nap1 as judged by immuno-blots and immuno-fluorescence (Figure 4C and D). However, C-Nap1 depletion did not trigger centrosome separation in the Plk1-inhibited cells (Figure 4E), suggesting additional requirements for Plk1 in the separation mechanism following disjunction.

Interphase Cdks and Plk1 collaborate to trigger centrosome localization of Eg5 in G2 phase

We next investigated how Cdks and Plk1 regulate Eg5 in G2 and M phase. A key event in the initiation of centrosome separation is the phosphorylation of Eg5 in its C-terminal tail domain at Thr927 stimulating its binding to MTs and localization at the mitotic spindle (Blangy *et al*, 1995; Sawin and Mitchison, 1995; Cahu *et al*, 2008). Mitotic Cdk1 is thought to be responsible for this phosphorylation. However, we observed that Eg5 mediates centrosome separation independently of Cdk1. This prompted us to probe the phosphorylation of Eg5 after Cdk1 inhibition using a P-Thr927 phospho-specific antibody (Materials and methods). We confirmed that this antibody only cross-reacted with phosphorylated Eg5 (Supplementary Figure S3A and B) and used it to compare Eg5 phosphorylation in Cdk1-inhibited and mitotic cells (DT40 *cdk1as* cells in Figure 5A; *HeLa* cells in Supplementary Figure S3C). Surprisingly, we found that the majority of Eg5 was already phosphorylated at Thr927 despite Cdk1 inhibition in both human and chicken cells. There was no major increase in phosphorylation in the released mitotic cells, but phosphorylation levels dropped significantly as cells progressed into G1 phase (Figure 5A). Plk1 inhibition had no effect on Eg5 phosphorylation at Thr927 (Figure 5B) suggesting that the kinase is not involved in this control pathway.

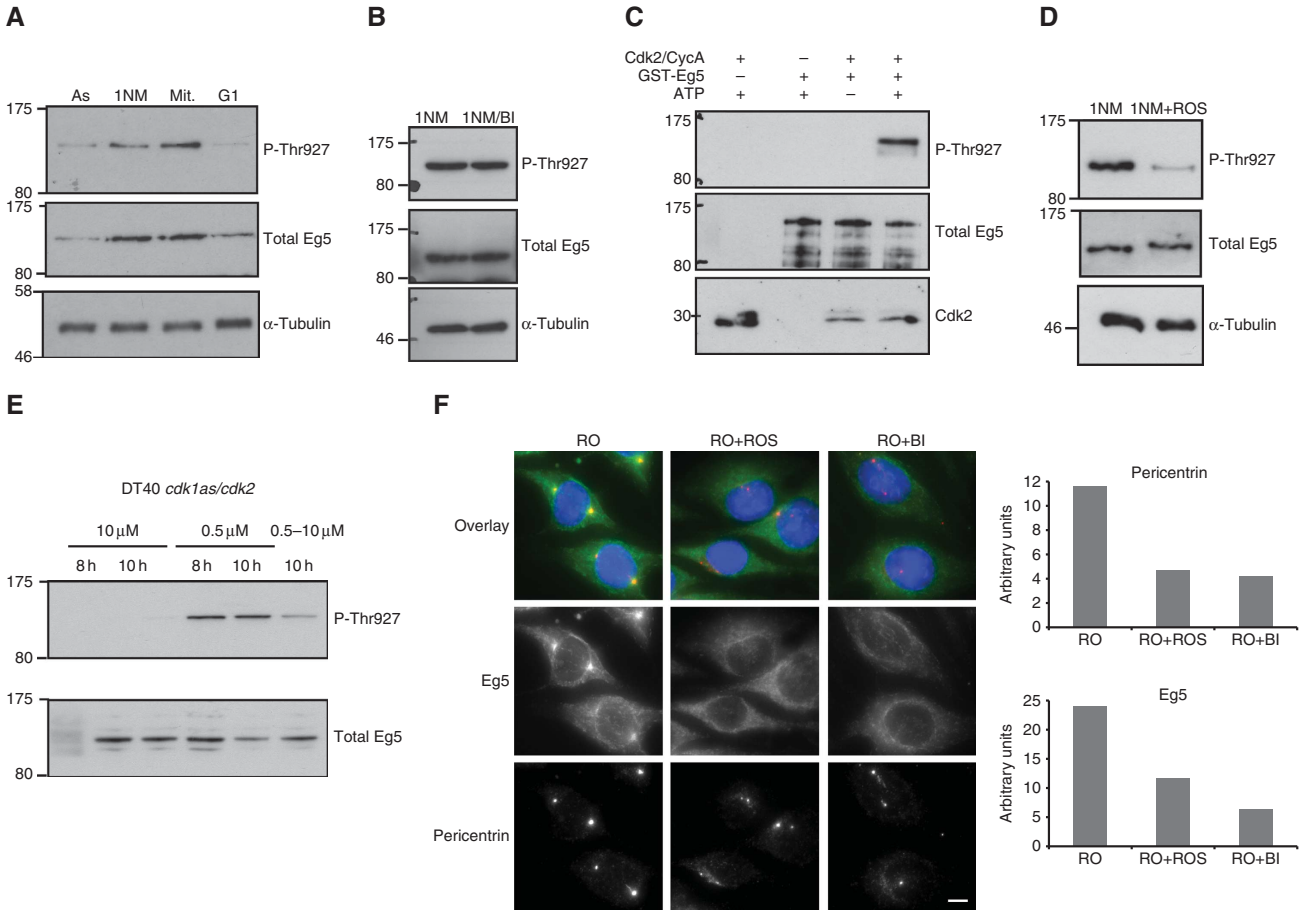

Figure 5 Eg5 phosphorylation in G2 and M phase. (**A**) Immuno-blots probing extracts of *cdk1as* cells at different cell-cycle stages with the indicated antibodies. As: asynchronous cells; 1NM: *cdk1as* cells treated for 6 h with 1NMPP1; Mit: cells released for 30 min from the 1NMPP1 arrest; G1: cells released for 90 min from the 1NMPP1 arrest. (**B**) Immuno-blots with the indicated antibodies of DT40 extracts. *cdk1as* cells were treated with 10 μM 1NMPP1 (1NM) or co-treated with 10 μM 1NMPP1 and 100 nM BI2536 for 6 h (1NM/BI). (**C**) Kinase assays using bacterially expressed recombinant GST-Eg5 and Cdk2/cyclinA probed with Eg5, and phospho-specific Eg5 P-Thr 927 antibodies. (**D**) Immuno-blots probing extracts of DT40 cells with the indicated antibodies. *cdk1as* cells were treated for 6 h with 1NMPP1, and for an additional 2 h with or without 50 μM Roscovitine (1NM + ROS). (**E**) Immuno-blots probing extracts from *cdk1as/cdk2* DT40 cells subjected to the indicated treatments. Cells in the final lane had been treated for 8 h with 0.5 μM 1NMPP1 and shifted to 10 μM 1NMPP1 for another 2 h. (**F**) Immuno-fluorescent staining of *HeLa* cells with Eg5 and Pericentrin antibodies. Cells were treated for 22 h with 10 μM RO3306 (RO), and 50 μM Roscovitine or 100 nM BI2536 were added for the last 2 h (RO + ROS and RO + BI). Graphs show a quantification of the signal intensity of either antibody at the centrosomes using ImageJ analysis tools (for each sample $N > 100$).

Cdk2 is a likely candidate to compensate for Cdk1 to phosphorylate Eg5 on Thr927 in G2 phase. Accordingly, we confirmed that recombinant Cdk2/cyclin A phosphorylates Eg5 on Thr927 *in vitro* (Figure 5C). Moreover, further inhibition of both Cdk1 and Cdk2 by Roscovitine significantly reduced Thr927 phosphorylation in Cdk1-inhibited DT40 and *HeLa* cells (Figure 5D; Supplementary Figure S3D). We further probed the involvement of Cdk2 in Eg5 Thr927 phosphorylation by using a *cdk1as/cdk2* double mutant cell line (Hochegger *et al*, 2007). When treated with 10 μM 1NMPP1, these cells arrest in both G1 and G2 phases due to the requirement of Cdk1 in S-phase progression in the absence of Cdk2 (Supplementary Figure S3E). Under these circumstances, Eg5 Thr927 phosphorylation is abolished (Figure 5E), but this could be a secondary effect of the earlier cell-cycle arrest. A lower dose of 1NMPP1 allows enough Cdk activity for S-phase progression, but is still sufficient to block the mitotic functions of Cdk1 resulting in a G2 arrest (Supplementary Figure S3E). This dose of 1NMPP1 is also permissive for Thr927 phosphorylation (Figure 5E). However, a further shift to 10 μM 1NMPP1 in these G2-arrested cells causes a significant decrease in Thr927 phosphorylation (Figure 5E), while the same dose does not block Eg5 phosphorylation in G2 phase when Cdk2 is present (Figure 5A). Thus, either Cdk1 or Cdk2 can phosphorylate Eg5 at Thr927 in interphase.

To test what effect Cdk and Plk1 inhibition has on Eg5 localization, we probed *Hela* cells by immuno-fluorescence using Eg5 antibodies (Figure 5F). In Cdk1-inhibited cells, Eg5 is strongly enriched on centrosomes. When either Cdk2 or Plk1 activity is further inhibited in these cells, this centrosomal localization is lost, and at the same time centrosome maturation appears to be reversed as judged by decreased intensity of the signal from the anti-Pericentrin antibody. Thus, interphase Cdks and Plk1 cooperate to load Eg5 on the centrosomes prior to mitotic entry. However, Cdk1 could still further contribute to Eg5 activation via phosphorylation on sites other than Thr927. We searched for such novel sites in Eg5 by mass spectrometry (MS) analysis, but only detected the Thr927 phosphorylation event in Eg5 purified from either mitotic or G2-arrested *cdk1as* cells (Table I).

Table I Analysis of Eg5 by mass spectrometry

	Number of peptides	Coverage (%)	Modification
ETD			
1NM	22	18	Thr927
1NM/BI	23	22	Thr927
Rel	28	24	Thr927
CID			
1NM	50	44	Thr924/927
1NM/BI	52	46	Thr927
Rel	64	65	Thr927

Analysis of post-translational modification of Eg5 purified by large-scale immuno-precipitation from *cdk1as* cells collected after 6 h treatment with 10 μM 1NMPP1 (1NM), 10 μM 1NMPP1 and 100 nM BI2536 (1NM/BI) and 30 min after release from a 6-h arrest in 10 μM 1NMPP1 (Rel). Samples were analysed as described in Materials and methods. Electron transfer dissociation (ETD) and collision-induced dissociation (CID) were used for sample detection.

Depolymerization of the actin cytoskeleton inhibits the Eg5-opposing forces and increases the speed of centrosome separation in Cdk1-inhibited cells

Our analysis of Eg5 regulation suggests that this motor protein is already primed for action in G2 phase and may not be further activated by mitotic Cdk1. We thus shifted our attention to the Eg5-opposing forces that appear to hinder centrosome separation in G2 phase. First, we hypothesized that inactivation of Eg5 by inhibition of Plk1 or Cdk2 may shift the balance in favour for these opposing forces and cause already separated centrosomes to be pushed back together. We could detect such a reverse movement of centrosomes by live cell imaging (Figure 6A–C) and in cells fixed prior and post Plk1 or Cdk2 inhibition (Figure 6D; Supplementary Figure S3E). We hypothesized that the source of this Eg5-opposing activity could be related to the centrosome positioning forces that pull the centrosomes to the centre of interphase cells. An elegant model implies that this force is exerted via long and stable MTs that emanate from the centrosome and reach the actin cytoskeleton at the cell cortex (Burakov *et al*, 2003; Zhu *et al*, 2010). Thus, we tested the involvement of the actin polymers in force generation in our centrosome separation assay. For this purpose, we inhibited actin polymerization concomitantly with either Plk1 or Cdk activity in G2-arrested *cdk1as* cells and probed for reversal of centrosome separation. Strikingly, cytochalasin D, a potent inhibitor of actin polymerization, effectively abolished the reversal of centrosome separation under these circumstances (Figure 6D). This reverse force was also dependent on stable MTs and was inhibited by low doses of Nocodazole. Conversely, centrosomes were still pushed together after inhibition of Myosin 2 by Blebbistatin (Figure 6D).

Having found a way to inhibit the forces that reverse centrosome separation, we tested if we could speed up the dynamics of Plk1-dependent centrosome separation simply by relieving the centrosomes from this obstruction. We performed a similar block release experiment as described in Figure 2A, synchronizing the cells with unseparated centrosomes in G2 phase by Cdk1 and Plk1 inhibition. When we removed the Plk1 inhibitor from the medium, we could detect hardly any increase in centrosome separation in the first hour (Figures 2B and 6E). In marked contrast, the majority of centrosomes were widely separated within an hour in the presence of cytochalasin D. This separation was still dependent on Eg5 and was reversed by addition of Eg5 inhibitors (Figure 6E). Taken together, these data suggest that Eg5 is already primed for fast centrosome separation in G2 phase prior Cdk1 activation, but kept in check by forces that act on the centrosome via stable interphase MTs and depend on a stable actin cytoskeleton.

Increased dynamic instability of mitotic MTs is a regulatory element in the control of centrosome separation

It has long been known that MT dynamic instability is dramatically increased as cells enter mitosis (Wittmann *et al*, 2001), and Cdk1 has been shown to up-regulate MT dynamics in a number of model systems (Lamb *et al*, 1990; Verde *et al*, 1992; Moutinho-Pereira *et al*, 2009). Thus, the loss of long astral MTs following Cdk1 activation could contribute to the rapid and efficient centrosome separation

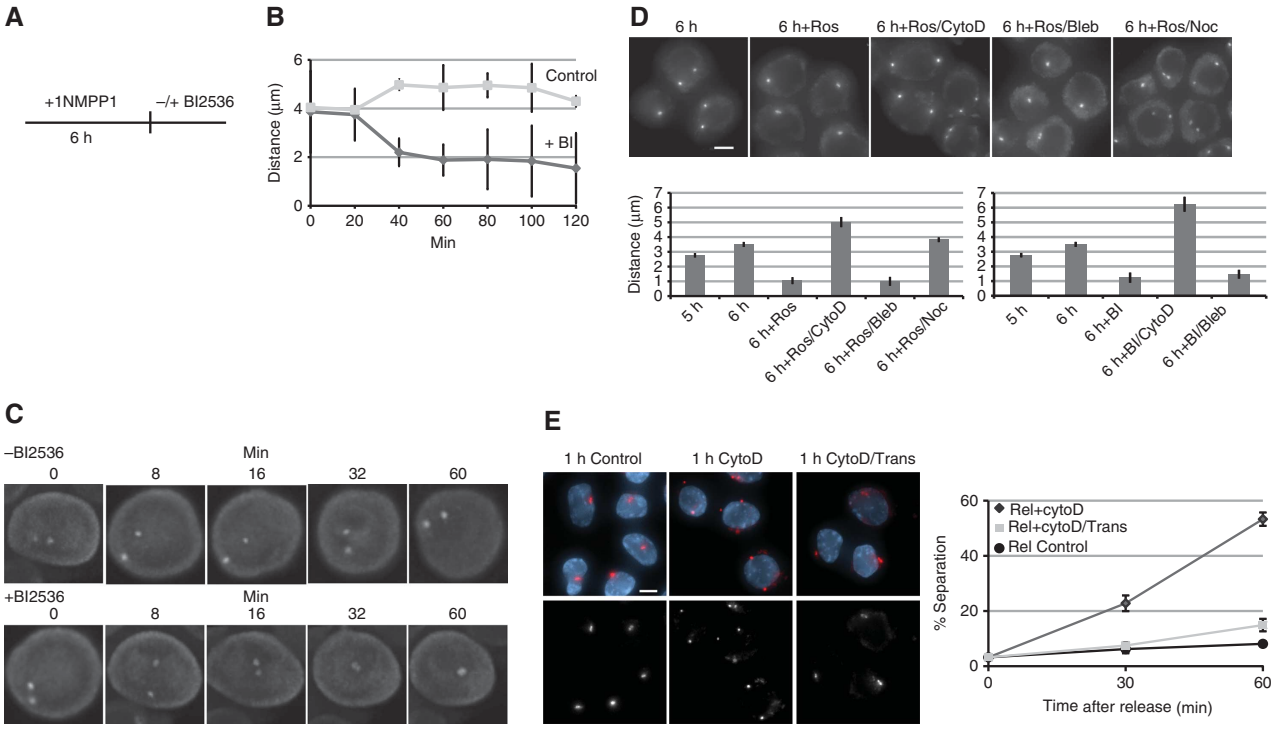

Figure 6 Plk1 inhibition results in reversal of centrosome separation in G2 phase. (**A**) Experimental set-up of Plk1 shut-off experiment. DT40 *cdk1as* cells are blocked in G2 with separated centrosomes by 6 h 10 μM 1NMPP1 treatment. At this time, 100 nM BI2536 was added to the cells and distances of centrosomes were scored by live cell imaging of GFP-γ-tubulin. (**B**) Quantitative analysis of time-lapse microscopy of BI2536-treated and control cells. Centrosome distances were measured in 20 cells every 20 min using Imaris 3D analysis tools. (**C**) 3D time-lapse microscopy of BI2536-treated and control cells expressing GFP γ-tubulin. The still images are MIPs of deconvolved 3D images (scale bar, 2 μm) from the time-lapse series (see also Supplementary Movies 04 and 05). (**D**) Centrosome collapse assay in fixed *cdk1as* cells probed by immunofluorescence with γ-tubulin antibodies. Cells were treated for 6 h with 0.5 μM 1NMPP1 and for the last hour additionally 50 μM Roscovitine or 100 nM BI2536 (6h + Ros and 6h + BI). In further samples, 10 μM CytochalasinD (CytoD), 50 μM Blebbistatin (Bleb) or 20 ng/ml Nocodazole (Noc) were added in parallel to the Plk1 and Cdk inhibitors. Mean centrosome distance was measured three times ($N > 100$ in each experiment) using Imaris. The images shown are MIPs from 3D stack images. (**E**) Dynamics of centrosome separation were assayed in a release experiment as described in Figure 2. *cdk1as* cells were treated for 6 h in 10 μM 1NMPP1 and 100 nM BI2536. Subsequently, BI2536 was washed out and centrosome separation was assayed at the indicated time points by γ-tubulin immuno-fluorescence. Following release from Plk1 inhibition, cells were treated with either DMSO (control), 10 μM cytochalasinD (CytoD) or 33 μM Trans24 (Trans). Centrosome separation was counted in three independent experiments using Imaris. The pictures shown are MIPS of 3D stack images.

that we observed in the cells released from Cdk1 inhibition. To test this hypothesis, we first confirmed that changes in MT dynamics occur following cdk1 activation in *cdk1as* cells. We probed *cdk1as* cells for MT nucleation activity before and after Cdk1 activation by depolymerizing MTs with high Nocodazole doses and observing MT repolymerization following removal of Nocodazole. Figure 7A shows that Cdk1-arrested (Cdk1off) cells displayed long astral MTs that reached from the centrosome to the cell periphery. In cells released from Cdk1 inhibition (Cdk1on), only very short MTs nucleated at the centrosomes. If this change in MT stability has indeed a role in the control of centrosome separation, we should see reduced separation in M phase but not G2 following MT stabilization; the opposite should be the case for MT destabilization, which should speed up separation in G2, but not in M phase. We tested this hypothesis by measuring distances of separated centrosomes after treatment with low doses of Nocodazole and Taxol. Figure 7B and C shows that MT stabilization with Taxol did indeed result in decreased separation in M but not G2 phase, while destabilization of MTs in a low Nocodazole dose did cause an increase in separation in G2-arrested cells but had little effect on M-phase cells.

Discussion

Our data suggest that centrosome separation is subjected to a complex interplay of controls and is already initiated in G2 phase by Plk1 and interphase Cdks, while being greatly enhanced by mitotic Cdk1 (see model in Figure 7). In agreement with previous studies (McCleland and O'Farrell, 2008; Gavet and Pines, 2010), we find that Cdk1 is not essential to allow the centrosomes to come apart in G2 phase before NEBD. We find that Plk1 activity is required for C-Nap1 displacement from the centrosomes in G2 phase, and that this disjunction step is slow and inefficient. Cdk1 activation significantly changes the timing of disjunction, with centrosomes coming apart within minutes of kinase activation independently of Plk1. Mardin *et al* (2010) recently reported a novel mechanism of centrosome disjunction that involves the regulation of Nek2 and C-Nap1 by Mst2 kinase. This pathway appeared to be only required when centrosome separation was slowed down by partial Eg5 inhibition. It is tempting to speculate that Plk1 could be linked to the Mst2-dependent pathway, while Cdk1 activation could cause an increase in the force of separation that is *per se* sufficient to quickly break the cohesion between the centrosomes.

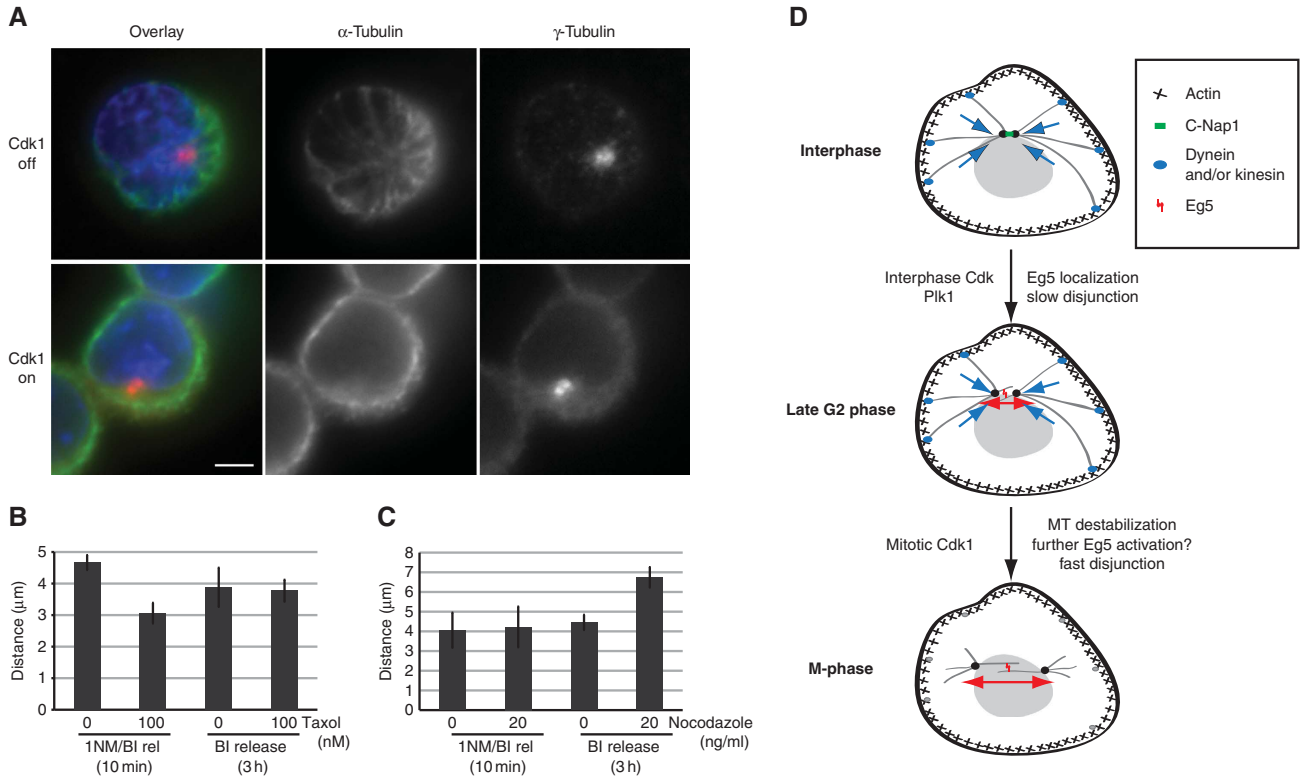

Figure 7 Dynamics of centrosome separation in G2 and M phase depend on MT stability. (**A**) MT nucleation assay in G2 and M phase *cdk1as* cells. The cells were treated for 6 h with 1NMPP1 to arrest in G2 phase and for a further 2 h 2 μg/ml Nocodazole was added to depolymerize all MTs (Cdk1off). The cells were released into M phase by 1NMPP1 removal (cdk1on). MT nucleation was assayed by immuno-fluorescence in cells fixed 5 min after Nocodazole removal from the media. (**B**) *cdk1as* cells were treated for 6 h with 10 μM 1NMPP1 and 100 nM BI2536, and 10 nM Taxol was added for the last 30 min of the block. Following release from either both 1NMPP1 (1NM/BI release) and BI2536 (BI release), cells were kept for the indicated time in Taxol and then centrosome separation was assayed by γ-tubulin immuno-fluorescence using Imaris. Shown are the mean distances of separated centrosomes. (**C**) As in (**B**) using 20 ng/ml Nocodazole. (**D**) Model. In interphase, centrosomes are pushed into the cell centre by forces coming from radial MT that connect to the cell cortex. The force is generated by cortical dynein (pulling force), and/or an unknown kinesin (pushing force). In G2 phase, Cdk2 and Plk1 trigger Eg5 enrichment at the centrosome. Plk1 also triggers centrosome disjunction via C-Nap1 displacement. However, the Eg5 obstructing forces still prevail and delay separation. Cdk1 activation triggers an increase in MT depolymerization, thereby releasing the centrosome from the Eg5 counteracting forces and allowing Eg5 to push the centrosomes rapidly apart.

Once disjunction has occurred, Eg5 is able to push the centrosomes apart both before and after Cdk1 activation, albeit with greatly different dynamics. Both Plk1 and interphase Cdk1/2 activity contributes to Eg5 enrichment at the centrosome. Cdk1/2 regulate this step via Thr927 phosphorylation, which stimulates MT binding (Cahu *et al*, 2008). Plk1 does not appear to phosphorylate Eg5 *in vitro* (Hochegger Laboratory, unpublished results), and Plk1 inhibition does not appear to affect the phosphorylation of Eg5 at Thr927 but controls accumulation of pericentriolar material in G2 phase in concert with interphase Cdks (Figure 5F). However, a functional correlation between centrosome maturation and Eg5 recruitment has yet to be established. In principle, Eg5 should move towards the plus end of the MTs and it remains to be clarified how Eg5 is actually retained and concentrated at the minus end of MTs at the centrosome. We did not find any evidence that Cdk1 further modifies Eg5 and accordingly Blangy *et al* (1995) showed that Thr927 was the only Cdk phosphorylation site in the protein. However, we cannot exclude that Cdk1 also exerts additional control on Eg5 in M phase.

The dramatic increase in the velocity of centrosome separation after Cdk1 activation may thus be a result, not of Eg5 activation, but of the removal of the force that opposes separation. This obstruction of separation becomes apparent when either Cdks or Plk1 is inhibited in G2 phase, most likely because of the inactivation of Eg5. Conversely, Eg5 inhibition in mitosis does not result in spindle pole collapse in mitotic cells (Kapoor *et al*, 2000). The minus-end-directed motor protein Dynein (Tanenbaum *et al*, 2008; Ferenz *et al*, 2009) as well as the Tiam1, Rac signalling pathway (Woodcock *et al*, 2010) have been implicated in this force generation. Interestingly, Dynein has also been proposed to generate force on the long astral interphase MTs that connect the centrosome to the cell cortex (Burakov *et al*, 2003; Zhu *et al*, 2010). These forces are thought to ensure the positioning of the centrosome in the cell centre. In this study, we provide evidence that actin polymers as well as stable MTs are required to generate the force that reverses centrosome separation in G2 phase. Myosin does not appear to be involved in force generation, but the actin cytoskeleton may simply serve as a matrix that MT-dependent motors use to push or pull on the centrosome. The Dynein/Dynactin complex that cross-links MTs to actin is a likely candidate to generate this force by providing a balanced pulling force from all directions. Force could also be generated by a kinesin pushing towards the plus end, or simply from MT polymerization as demonstrated *in vitro* (Holy *et al*, 1997).

Strikingly, it appears to be sufficient to remove this obstruction to centrosome separation by depolymerizing the actin cytoskeleton, to considerably increase the efficiency of Plk1-dependent centrosome separation in G2 phase (Figure 6). This result suggests that Eg5 is ready for action prior to Cdk1 activation, but kept in check by the opposing force. It is thus likely that Cdk1 triggers fast separation by breaking the Eg5-opposing force. Our results in Figure 7 suggest that destabilization of the long interphase MTs by Cdk1 has a critical role in this step. However, Cdk1 could also contribute to modulation of Dynein motor activity and to rearrangements in the actin cytoskeleton.

The question remains why such a differentially controlled mechanism for centrosome separation has evolved. Gavet and Pines (2010) have shown in a series of elegant experiments that in an unperturbed cell cycle, centrosome separation coincides with Cdk1 activation. However, manipulation of cell-cycle progression by synchronization led to uncoupling of Cdk1 activity and centrosome separation. Plk1-triggered centrosome separation may thus only become apparent when cell-cycle progression has been delayed. Such a delay may, for example, occur in response to DNA damage, or other obstacles to cell-cycle progression. Under these circumstances, it could be desirable to prepare the cells for mitotic entry even in the absence of Cdk1 activity by triggering centrosome separation. It is noteworthy that Plk1 also provides alternative mechanisms for loss of chromosome cohesion (Alexandru *et al*, 2001) and centriole disengagement (Tsou *et al*, 2009). In both cases, Plk1 acts in parallel with Separase to provide an independent way of achieving loss of cohesion between sister chromatids and centrioles. Thus, a function for Plk1 to control back-up pathways appears to be a common theme during mitosis. Our results suggest that such a function also exists in regulating centrosome separation.

Materials and methods

Chemicals and biochemicals

All chemicals were obtained from Fisher Scientific or Sigma-Aldrich unless otherwise stated. 1NMPP1 was synthesized following published procedures (Bishop *et al*, 1999). 3MBPP1 was a kind gift from Prasad Jallepalli (Memorial Sloan-Kettering Cancer Center, New York, USA). Recombinant Cdk1/cyclinA was a kind gift from Tim Hunt (Clare Hall Laboratories, London, UK) Protease and phosphatase inhibitor (Phos-stop) cocktails were from Roche Diagnostics, West Sussex, UK. Protein G Dynabeads and ProLong® Gold with DAPI were purchased from Invitrogen Ltd, Paisley, UK. Bio-Rad protein assay reagent was obtained from Bio-Rad Laboratories Ltd, Hertfordshire, UK. RO3306 and MG132 were purchased from Merck Chemicals Ltd, Nottingham, UK. BI2536 was purchased from Axon Medchem. Trans24 was bought from Axxora Ltd, Nottingham, UK. Plasmids expressing GST-Eg5 was a gift from Ann Blangy and Frank Kozielski.

Cell culture, synchronization and inhibitor treatments

Chicken DT40 cells including *cdk1as* cells were cultured as previously described (Hochegger *et al*, 2007). For Cdk1 inhibition, cells were treated with 10 μM 1NMPP1 for 6 h; in the case of GFP-γ-tubulin-expressing cells, this was extended to 8 h to compensate for slower growth of these cells (data not shown). To inhibit Plk1, 100 nM BI2536 was added to the media for 6 h. To inhibit Eg5, 33 μM Trans24 was added to media for 6 h. For release experiments, cells were then rinsed with 3 × 50 ml RPMI media containing indicated drugs and cultured further for indicated time points. To obtain mitotic DT40 cells, cells were collected after 30 min of release and for G1 cells, 90 min after release. Mitotic enrichment for immuno-precipitation experiments was performed by adding 0.1 μg/ml Nocodazole to cells for 4 h. Elutriation of DT40 cells was performed as described previously (Takata *et al*, 1998).

HeLa cells were cultured in Dulbecco's modified Eagle Medium supplemented with 10% FCS, 2 mM L-glutamine, 100 U/ml penicillin and 0.1 mg/ml streptomycin in a 37 °C, 5% CO_2 incubator. To inhibit Cdk1 activity, cells were treated with 7.5 μM RO3306 to 10 μM for 20 h. We found significant batch-to-batch variation in the effect of RO3306, with some batches causing a G1 arrest at 10 μM; in these cases, we reduced the dose to 7.5 μM to obtain a G2 arrest. To inhibit Plk1, 100 nM BI2536 was added to the media for 20 h and for Eg5 inhibition 100 nM STLC was added to media for 20 h. For roscovitine treatments, DT40 cells were treated with 10 μM 1NMPP1 for 6 h followed by 2 h with the addition of 50 μM roscovitine. For roscovitine treatments, HeLa cells were treated with 7.5 μM RO3306 for 20 h followed by 4 h with the addition of 50 μM roscovitine.

Plk1WT-RPE or *Plk1as*-RPE cells were a kind gift of Prasad Jallepalli and cultivated as described (Burkard *et al*, 2007). To inhibit Cdk1 in this cell line, 5 μM RO3306 was added to the media and to inhibit the *Plk1as* mutant 20 μM 3MBPP1 was added for 20 h.

Antibodies

Primary antibodies used for this study were generally bought from Abcam and were used at manufacturers' recommended concentrations. Centrin-2 rabbit polyclonal was a gift from Elmar Schiebel; Alexa-fluor®-conjugated secondary antibodies for immunostaining or FACS analysis; Alexa488 anti-rabbit, Alexa488 anti-mouse and Alexa594 anti-rabbit were purchased from Invitrogen and HRP-conjugated rabbit or mouse polyclonal secondary antibodies for western blotting were from Dakocytomation Ltd, Cambridge, UK.

Immuno-fluorescence, microscopy and image analysis

Hela and RPE cells were grown on coverslips and fixed for 10 min in 3.7% formaldehyde, rinsed 4 × in PBS and fixed in methanol for 10 min at −20 °C. DT40 cell suspension cultures ($\sim 5 \times 10^4$ cells per 0.1 ml) were spun onto slides at 1000 r.p.m. for 3 min using a cell spin cytocentrigfuge from Tharmac. Cells were then fixed using 3.7% formaldehyde for 10 min. Slides or coverslips were then rinsed in PBS and cells permeabilized in PBS-0.1% NP40. Cells were blocked in 1% BSA for 30 min and probed with primary antibodies (as indicated in figure legends) for 30 min–1 h. Slides/coverslips were rinsed 4 × in PBS and probed with Alexa secondary antibodies listed below for 30 min to 1 h. Slides/coverslips were then rinsed 4 × in PBS and coverslips were mounted using ProLong® Gold mounting solution containing DAPI (Invitrogen). For standard image acquisition, a personal Delta Vision® microscope equipped with a UPLS apo, N.A. 1.4, × 100 oil immersion objective (Olympus), standard filter sets (excitation 360/40; 490/20; 555/28; emission 457/50; 528/38; 617/40) and a Cascade EMCCD camera (Roper scientific). *Z*-series of 0.3 μm stacks were acquired using SoftWorx software (Version 3.7.1) and deconvolution performed using SVI Huygens Professional Deconvolution Software (Version 3.5). Maximum intensity projections were obtained in Omero (Version Beta 4.1.1) and exported as Tiff files. For centrosome separation and distance analysis, images were acquired on the Delta Vision® microscope with × 100 or × 60 (PlAPON, 1.42 NA) oil immersion objective as described above. Delta Vision files were imported into Imaris software (Bitplane, Version 6.3.0) for 3D distance measurements. Measurements were then exported to Excel and plotted.

Where indicated, an Olympus Scan-R (Version 2.1) automated image acquisition microscope with × 40 oil immersion objective (UPLFLN, N.A. 1.3) was used to acquire images and to quantify and analyse the number of γ-tubulin spots (centrosomes) per nuclei (DAPI) using the ScanR® analysis software. We set up the analysis so that pairs of centrosomes with distances > 0.5 μm were scored as separated. Image gating and edge detection was performed according to the manufacturers' protocols.

Live cell imaging

Cdk1as cells were stably transfected with GFP γ-tubulin in an IresPuroexpression vector (a gift from Toru Hirota, Cancer Centre, Tokyo). Note that these cells already express GFP (Hochegger *et al*, 2007), so that both the entire cell, as well as the centrosomes can be visualized. Time-lapse microscopy was performed on concavalin-coated coverglass chambers (Nunc) in CO_2-independent medium (Invitrogen) in an environmental chamber heated to 39 °C using a personal DeltaVision® microscope and a × 100 oil immersion objective as described above with GFPO filters (excitation 470/40;

emission 520/40). A total of 0.4 μM stacks were taken 60 times at either 30 s, or 2 min intervals using 1%, or 10% neutral density filters and × 100 gain on the EMCCD camera. The 3D time series was deconvolved using Huygens Professional Deconvolution software and analysed in Imaris. Maximum intensity projections of the time series were exported into Quicktime format for presentation as Supplementary Movies. For velocity calculations, we calculated the ratio of the distance travelled in each time step and the length of each time step. We only included data for distances above 2 μm to focus on separation dynamics after successful disjunction. The mean of the instantaneous separation velocities was calculated for each run, and the mean and s.d. of the data from five runs are shown.

Preparation of total cell extracts, immuno-blotting, immuno-precipitation, phosphatase treatments and in vitro phosphorylation assays

For cell lysate preparation, 10^6 DT40 cells or $1–5 \times 10^5$ *HeLa* or RPE cells were washed once in PBS and lysed in 50 μl ECB buffer (50 mM Tris pH 7.5, 120 mM NaCl, 0.5% NP40, 1 mM EDTA, 0.05% β-mercaptoethanol and protease (1 tablet/50 ml) and phosphatase (1 tablet per 10 ml) inhibitors), incubated on ice for 20 min. Cells were sonicated, cell debris was then cleared by centrifugation at 13 000 r.p.m., 10 min at 4 °C and the supernatants were transferred to fresh tubes. Protein concentrations were determined by Bradford method and lysates were equalized for protein concentration using ECB buffer. For immuno-precipitation, cells were lysed in 500 μl IP lysis buffer (20 mM Tris pH 7.5, 137 mM NaCl, 10% glycerol, 1% triton, 2 mM EDTA, 0.05% β-mercaptoethanol, protease and phosphatase inhibitors (as above)). Lysates were sonicated, cleared and equalized as above. Lysates were incubated with 3–5 μg Myc or Eg5 antibody (as indicated in figure legends) at 4 °C for 1 h with end over end rotation and 20 μl of Protein G Dynabeads® were added to precipitated proteins. Samples were incubated at 4 °C for a further 2 h. Beads were then rinsed with 3 × 1 ml IP lysis buffer. Beads were then re-suspended in 1 × SDS–PAGE sample buffer (12.5 mM Tris–HCl pH 6.8, 1.4% (w/v) SDS, 4% sucrose (w/v), 0.002% (w/v) bromophenyl blue, 0.4 mM β-mercaptoethanol) or prepared for kinase assays or phosphatase treatment. For Eg5 kinase assays, immuno-precipitates were washed once in 1 ml kinase assay buffer (50 mM MOPS, pH 7.5, 5 mM $MgCl_2$, 0.4 mM EGTA, 2 mM EDTA and protease/phosphatase tablets (as described above)). Beads were then re-suspended in 20 μl kinase assay buffer. To each reaction, 0.2 μg/μl bacterially expressed recombinant GST-Eg5 was added, and to start reactions, 10 μl of 100 μM ATP (made up in kinase assay buffer) was added. Reactions were incubated at 37 °C for 20 min and were terminated with the addition of 15 μl 5 × SDS–PAGE sample buffer and boiling at 95 °C for 5 min. *In vitro* kinase assays using recombinant CDK2/cyclinA at 40 ng/μl with 0.2 μg/μl GST-Eg5 were started by adding 25 μM ATP. Reactions were incubated at 37 °C for 20 min and were terminated with the addition of 15 μl 5 × SDS–PAGE sample buffer and boiling at 95 °C for 5 min. For phosphatase treatments, cells were lysed in phosphatase inhibitor-free IP lysis buffer, immuno-precipitated proteins were then rinsed twice in 500 μl phosphatase buffer (50 mM HEPES, pH 7.5, 100 mM NaCl, 2 mM DTT, 0.01% Brij-35 and 1 mM $MnCl_2$) and re-suspended in 20 μl phosphatase buffer. To one tube, 1 μl of calf immune alkaline phosphatase (Sigma) was added and reactions incubated at 30 °C for 1 h. Reactions were stopped by the addition of SDS–PAGE sample buffer and boiling at 95 °C for 5 min. Samples were then analysed by western blotting.

SiRNA transfections

HeLa cells were seeded in six-well plates at a density of 0.4×10^5 cells/ml and 24 h later were transfected with 20 nM control siRNA for human GAPDH 3 (FlexiTube siRNA (Qiagen) target sequence: AAGGTCGGAGTCAACGGATTT) or 20 nM C-NAP1 mix (FlexiTube siRNA target sequences: CACGGTCGCCTTCTCAGTCTA, CAGCTTCGACTGCACATGGAA), using HiPerFect transfection reagent (Qiagen) following the manufacturers' protocol; 30 h later cells were treated with 10 μM RO3306 (Cdk1) and 100 nM BI2536 (Plk1) inhibitors, where indicated. Cells were then prepared for immuno-fluorescence or western blotting as described.

Large-scale immuno-precipitation for MS

A total of 5×10^8 DT40 *cdk1as* cells were treated for 6 h with 10 μM 1NMPP1 (to inhibit CDK1) with or without 100 nM BI2536 (Plk1 inhibitor). For mitotic extracts, 1NMPP1 blocked cells were then released as described in the release protocol for 30 min. Cell pellets were then rinsed in PBS and re-suspended in IP lysis buffer. Lysates were sonicated, cleared and then equalized by Bradford method. In all, 1 ml batches of lysates were incubated with 5 μg of Eg5 antibody at 4 °C and immuno-precipitation performed as above. Beads were pooled and re-suspended in 70 μl NuPAGE 1 × sample buffer (Invitrogen) containing reducing agent. Samples were subjected to electrophoresis on 4–12% Bis–Tris minigels (Invitrogen), with MOPs running buffer. Gels were fixed and stained with colloidal blue stain (Invitrogen) as per manufacturers' protocol. Eg5 bands (as judged from parallel western blot analysis) were excised and prepared for tryptic digestion and MS.

Mass spectrometry

Gel slices (1–2 mm) were prepared for mass spectrometric analysis using the Janus liquid handling system (Perkin-Elmer, UK). Gel pieces were destained with 50% v/v acetonitrile and 50 mM ammonium bicarbonate, reduced with 10 mM DTT and alkylated with 55 mM iodoacetamide. After alkylation, proteins were digested with 6 ng/μl Trypsin (Promega, UK) overnight at 37 °C. Peptides were extracted in 2% v/v formic acid and 2% v/v acetonitrile. The digest was analysed by nano-scale capillary LC–MS/MS using a nanoAcquity UPLC (Waters, UK). A C18 symmetry 5 μm, 180 μm × 20 mm μ-Precolumn (Waters, UK), trapped the peptides prior to separation on a C18 BEH130 1.7 μm, 75 μm × 100 mm analytical UPLC column (Waters, UK). Peptides were eluted with a gradient of acetonitrile. The analytical column outlet was directly interfaced via a modified nano-flow electrospray ionization source, with a hybrid linear quadrupole Fourier transform mass spectrometer (LTQ Orbitrap XL/ETD, ThermoScientific, San Jose). Data-dependent analysis was carried out using a resolution of 30 000 for the full MS spectrum, followed by eight MS/MS spectra in the linear ion trap. LC–MS/MS data were then searched against a protein database (UniProt KB) using the Mascot search engine programme (Matrix Science, UK) allowing for variable modifications including phosphorylated residues. MS/MS data were validated using the Scaffold programme (Proteome Software Inc.).

FACS analysis

Cells were trypsinized, spun down, washed once with PBS and then fixed using 70% EtOH. Cells were centrifuged at 1500 r.p.m. for 3 min and rinsed in 0.5 ml of 3% BSA solution, re-centrifuged and re-suspended in 0.5 ml 3% BSA solution containing 1 μg/ml RNAse A and 5 μg/ml propidium iodide. Cells were then analysed for DNA content using an FACSCanto (BD Biosciences) and FACS Diva software to plot PI area versus cell counts.

Supplementary data

Supplementary data are available at *The EMBO Journal* Online (http://www.embojournal.org).

Acknowledgements

We thank Drs Prasad Jallepalli, Tim Hunt, Ann Blangy, Frank Kozielski and Elmar Schiebel for contributing reagents and Mr Gig Ahlstrand for technical assistance with the TEM. HH and NH were funded by a Wellcome Trust Career Development Fellowship (082267/Z/07/Z), ES by a CRUK project Grant (C28206, A9057) and RK by a NIH Grant NIH R01 GM55735).

Author contributions: ES designed and performed experiments in Figure 1–6; NH performed experiments in Figure 7; CV performed experiments in Figure 1; IR performed data analysis in Figure 3; CL and HS synthesized 1NMPP1; KS helped setting up 3D image analysis; HF and MS performed mass spectrometry; TH helped setting up live cell imaging analysis; RK performed electron microscopy (Supplementary Figure S1); HH conceptualized the study, designed and performed experiments.

Conflict of interest

The authors declare that they have no conflict of interest.

References

Alexandru G, Uhlmann F, Mechtler K, Poupart MA, Nasmyth K (2001) Phosphorylation of the cohesin subunit Scc1 by Polo/Cdc5 kinase regulates sister chromatid separation in yeast. *Cell* **105:** 459–472

Bahe S, Stierhof YD, Wilkinson CJ, Leiss F, Nigg EA (2005) Rootletin forms centriole-associated filaments and functions in centrosome cohesion. *J Cell Biol* **171:** 27–33

Basto R, Brunk K, Vinadogrova T, Peel N, Franz A, Khodjakov A, Raff JW (2008) Centrosome amplification can initiate tumorigenesis in flies. *Cell* **133:** 1032–1042

Bishop AC, Kung C, Shah K, Witucki L, Shokat KM, Liu Y (1999) Generation of monospecific nanomolar tyrosine kinase inhibitors via a chemical genetic approach. *J Am Chem Soc* **121:** 627–631

Blagden SP, Glover DM (2003) Polar expeditions—provisioning the centrosome for mitosis. *Nat Cell Biol* **5:** 505–511

Blangy A, Lane HA, d'Herin P, Harper M, Kress M, Nigg EA (1995) Phosphorylation by p34cdc2 regulates spindle association of human Eg5, a kinesin-related motor essential for bipolar spindle formation *in vivo*. *Cell* **83:** 1159–1169

Bornens M, Paintrand M, Berges J, Marty MC, Karsenti E (1987) Structural and chemical characterization of isolated centrosomes. *Cell Motil Cytoskeleton* **8:** 238–249

Burakov A, Nadezhdina E, Slepchenko B, Rodionov V (2003) Centrosome positioning in interphase cells. *J Cell Biol* **162:** 963–969

Burkard ME, Randall CL, Larochelle S, Zhang C, Shokat KM, Fisher RP, Jallepalli PV (2007) Chemical genetics reveals the requirement for Polo-like kinase 1 activity in positioning RhoA and triggering cytokinesis in human cells. *Proc Natl Acad Sci USA* **104:** 4383–4388

Cahu J, Olichon A, Hentrich C, Schek H, Drinjakovic J, Zhang C, Doherty-Kirby A, Lajoie G, Surrey T (2008) Phosphorylation by Cdk1 increases the binding of Eg5 to microtubules *in vitro* and in Xenopus egg extract spindles. *PLoS One* **3:** e3936

Casenghi M, Meraldi P, Weinhart U, Duncan PI, Korner R, Nigg EA (2003) Polo-like kinase 1 regulates Nlp, a centrosome protein involved in microtubule nucleation. *Dev Cell* **5:** 113–125

Castellanos E, Dominguez P, Gonzalez C (2008) Centrosome dysfunction in Drosophila neural stem cells causes tumors that are not due to genome instability. *Curr Biol* **18:** 1209–1214

DeBonis S, Skoufias DA, Lebeau L, Lopez R, Robin G, Margolis RL, Wade RH, Kozielski F (2004) *In vitro* screening for inhibitors of the human mitotic kinesin Eg5 with antimitotic and antitumor activities. *Mol Cancer Ther* **3:** 1079–1090

Ferenz NP, Paul R, Fagerstrom C, Mogilner A, Wadsworth P (2009) Dynein antagonizes eg5 by crosslinking and sliding antiparallel microtubules. *Curr Biol* **19:** 1833–1838

Fry AM, Mayor T, Meraldi P, Stierhof YD, Tanaka K, Nigg EA (1998) C-Nap1, a novel centrosomal coiled-coil protein and candidate substrate of the cell cycle-regulated protein kinase Nek2. *J Cell Biol* **141:** 1563–1574

Ganem NJ, Godinho SA, Pellman D (2009) A mechanism linking extra centrosomes to chromosomal instability. *Nature* **460:** 278–282

Gavet O, Pines J (2010) Progressive activation of CyclinB1-Cdk1 coordinates entry to mitosis. *Dev Cell* **18:** 533–543

Hagan I, Yanagida M (1992) Kinesin-related cut7 protein associates with mitotic and meiotic spindles in fission yeast. *Nature* **356:** 74–76

Heck MM, Pereira A, Pesavento P, Yannoni Y, Spradling AC, Goldstein LS (1993) The kinesin-like protein KLP61F is essential for mitosis in Drosophila. *J Cell Biol* **123:** 665–679

Hochegger H, Dejsuphong D, Sonoda E, Saberi A, Rajendra E, Kirk J, Hunt T, Takeda S (2007) An essential role for Cdk1 in S phase control is revealed via chemical genetics in vertebrate cells. *J Cell Biol* **178:** 257–268

Holy TE, Dogterom M, Yurke B, Leibler S (1997) Assembly and positioning of microtubule asters in microfabricated chambers. *Proc Natl Acad Sci USA* **94:** 6228–6231

Hoyt MA, He L, Loo KK, Saunders WS (1992) Two Saccharomyces cerevisiae kinesin-related gene products required for mitotic spindle assembly. *J Cell Biol* **118:** 109–120

Kapoor TM, Mayer TU, Coughlin ML, Mitchison TJ (2000) Probing spindle assembly mechanisms with monastrol, a small molecule inhibitor of the mitotic kinesin, Eg5. *J Cell Biol* **150:** 975–988

Lamb NJ, Fernandez A, Watrin A, Labbe JC, Cavadore JC (1990) Microinjection of p34cdc2 kinase induces marked changes in cell shape, cytoskeletal organization, and chromatin structure in mammalian fibroblasts. *Cell* **60:** 151–165

Lane HA, Nigg EA (1996) Antibody microinjection reveals an essential role for human polo-like kinase 1 (Plk1) in the functional maturation of mitotic centrosomes. *J Cell Biol* **135:** 1701–1713

Le Guellec R, Paris J, Couturier A, Roghi C, Philippe M (1991) Cloning by differential screening of a Xenopus cDNA that encodes a kinesin-related protein. *Mol Cell Biol* **11:** 3395–3398

Lenart P, Petronczki M, Steegmaier M, Di Fiore B, Lipp JJ, Hoffmann M, Rettig WJ, Kraut N, Peters JM (2007) The small-molecule inhibitor BI 2536 reveals novel insights into mitotic roles of polo-like kinase 1. *Curr Biol* **17:** 304–315

Lim HH, Zhang T, Surana U (2009) Regulation of centrosome separation in yeast and vertebrates: common threads. *Trends Cell Biol* **19:** 325–333

Mardin BR, Lange C, Baxter JE, Hardy T, Scholz SR, Fry AM, Schiebel E (2010) Components of the Hippo pathway cooperate with Nek2 kinase to regulate centrosome disjunction. *Nat Cell Biol* **12:** 1166–1176

Mayor T, Hacker U, Stierhof YD, Nigg EA (2002) The mechanism regulating the dissociation of the centrosomal protein C-Nap1 from mitotic spindle poles. *J Cell Sci* **115:** 3275–3284

Mayor T, Stierhof YD, Tanaka K, Fry AM, Nigg EA (2000) The centrosomal protein C-Nap1 is required for cell cycle-regulated centrosome cohesion. *J Cell Biol* **151:** 837–846

McCleland ML, O'Farrell PH (2008) RNAi of mitotic cyclins in Drosophila uncouples the nuclear and centrosome cycle. *Curr Biol* **18:** 245–254

McInnes C, Mazumdar A, Mezna M, Meades C, Midgley C, Scaerou F, Carpenter L, Mackenzie M, Taylor P, Walkinshaw M, Fischer PM, Glover D (2006) Inhibitors of Polo-like kinase reveal roles in spindle-pole maintenance. *Nat Chem Biol* **2:** 608–617

Meraldi P, Nigg EA (2002) The centrosome cycle. *FEBS Lett* **521:** 9–13

Mountain V, Simerly C, Howard L, Ando A, Schatten G, Compton DA (1999) The kinesin-related protein, HSET, opposes the activity of Eg5 and cross-links microtubules in the mammalian mitotic spindle. *J Cell Biol* **147:** 351–366

Moutinho-Pereira S, Debec A, Maiato H (2009) Microtubule cytoskeleton remodeling by acentriolar microtubule-organizing centers at the entry and exit from mitosis in Drosophila somatic cells. *Mol Biol Cell* **20:** 2796–2808

Oshimori N, Ohsugi M, Yamamoto T (2006) The Plk1 target Kizuna stabilizes mitotic centrosomes to ensure spindle bipolarity. *Nat Cell Biol* **8:** 1095–1101

Paintrand M, Moudjou M, Delacroix H, Bornens M (1992) Centrosome organization and centriole architecture: their sensitivity to divalent cations. *J Struct Biol* **108:** 107–128

Petronczki M, Lenart P, Peters JM (2008) Polo on the rise-from mitotic entry to cytokinesis with Plk1. *Dev Cell* **14:** 646–659

Roof DM, Meluh PB, Rose MD (1992) Kinesin-related proteins required for assembly of the mitotic spindle. *J Cell Biol* **118:** 95–108

Rosenblatt J (2005) Spindle assembly: asters part their separate ways. *Nat Cell Biol* **7:** 219–222

Sawin KE, LeGuellec K, Philippe M, Mitchison TJ (1992) Mitotic spindle organization by a plus-end-directed microtubule motor. *Nature* **359:** 540–543

Sawin KE, Mitchison TJ (1995) Mutations in the kinesin-like protein Eg5 disrupting localization to the mitotic spindle. *Proc Natl Acad Sci USA* **92:** 4289–4293

Sumara I, Gimenez-Abian JF, Gerlich D, Hirota T, Kraft C, de la Torre C, Ellenberg J, Peters JM (2004) Roles of polo-like kinase 1 in the assembly of functional mitotic spindles. *Curr Biol* **14:** 1712–1722

Sunder-Plassmann N, Sarli V, Gartner M, Utz M, Seiler J, Huemmer S, Mayer TU, Surrey T, Giannis A (2005) Synthesis and biological evaluation of new tetrahydro-beta-carbolines as inhibitors of the mitotic kinesin Eg5. *Bioorg Med Chem* **13:** 6094–6111

Sunkel CE, Glover DM (1988) polo, a mitotic mutant of Drosophila displaying abnormal spindle poles. *J Cell Sci* **89** (Part 1)**:** 25–38

Takata M, Sasaki MS, Sonoda E, Morrison C, Hashimoto M, Utsumi H, Yamaguchi-Iwai Y, Shinohara A, Takeda S (1998) Homologous recombination and non-homologous end-joining pathways of DNA double-strand break repair have overlapping roles in the maintenance of chromosomal integrity in vertebrate cells. *EMBO J* **17:** 5497–5508

Tanenbaum ME, Macurek L, Galjart N, Medema RH (2008) Dynein, Lis1 and CLIP-170 counteract Eg5-dependent centrosome separation during bipolar spindle assembly. *EMBO J* **27:** 3235–3245

Tsou MF, Wang WJ, George KA, Uryu K, Stearns T, Jallepalli PV (2009) Polo kinase and separase regulate the mitotic licensing of centriole duplication in human cells. *Dev Cell* **17:** 344–354

van Vugt MA, van de Weerdt BC, Vader G, Janssen H, Calafat J, Klompmaker R, Wolthuis RM, Medema RH (2004) Polo-like kinase-1 is required for bipolar spindle formation but is dispensable for anaphase promoting complex/Cdc20 activation and initiation of cytokinesis. *J Biol Chem* **279:** 36841–36854

Varis A, Salmela AL, Kallio MJ (2006) Cenp-F (mitosin) is more than a mitotic marker. *Chromosoma* **115:** 288–295

Vassilev LT, Tovar C, Chen S, Knezevic D, Zhao X, Sun H, Heimbrook DC, Chen L (2006) Selective small-molecule inhibitor reveals critical mitotic functions of human CDK1. *Proc Natl Acad Sci USA* **103:** 10660–10665

Verde F, Dogterom M, Stelzer E, Karsenti E, Leibler S (1992) Control of microtubule dynamics and length by cyclin A- and cyclin B-dependent kinases in Xenopus egg extracts. *J Cell Biol* **118:** 1097–1108

Wittmann T, Hyman A, Desai A (2001) The spindle: a dynamic assembly of microtubules and motors. *Nat Cell Biol* **3:** E28–E34

Woodcock SA, Rushton HJ, Castaneda-Saucedo E, Myant K, White GR, Blyth K, Sansom OJ, Malliri A (2010) Tiam1-Rac signaling counteracts Eg5 during bipolar spindle assembly to facilitate chromosome congression. *Curr Biol* **20:** 669–675

Xu N, Hegarat N, Black EJ, Scott MT, Hochegger H, Gillespie DA (2010) Akt/PKB supresses DNA damage response and checkpoint activation in late G2. *J Cell Biol* **190:** 297–305

Zhu J, Burakov A, Rodionov V, Mogilner A (2010) Finding the cell center by a balance of dynein and myosin pulling and microtubule pushing: a computational study. *Mol Biol Cell* **21:** 4418–4427